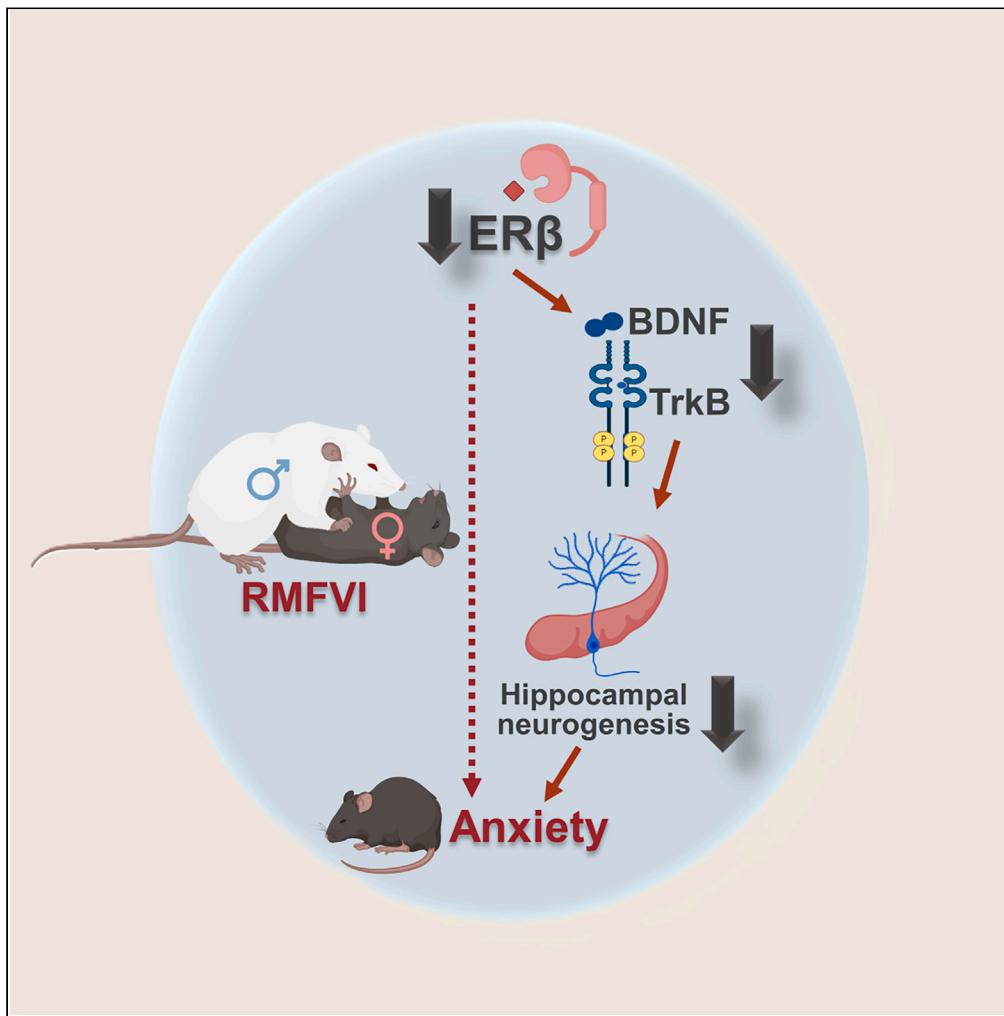


Article

Reiterated male-to-female violence disrupts hippocampal estrogen receptor  $\beta$  expression, prompting anxiety-like behavior



Jacopo Agrimi,  
Lucia Bernardele,  
Naeem Sbaiti, ...,  
Claudia Lodovichi,  
Marco Dal  
Maschio,  
Nazareno Paolucci

marco.dalmaschio@unipd.it  
(M.D.M.)  
npaoloc1@jhmi.edu (N.P.)

Highlights

Male violence impairs  
female hippocampal  
neurogenesis, triggering  
anxiety-like behavior

Male violence curtails  
hippocampal estrogen  
receptor  $\beta$  (ER $\beta$ ) and BDNF  
levels in females

Female ER $\beta$  KO mice die  
prematurely when  
subjected to reiterated  
male violence

Antagonizing hippocampal  
ER $\beta$  enhances anxiety in  
control female mice

Agrimi et al., iScience 27,  
110585  
September 20, 2024 © 2024  
Published by Elsevier Inc.  
[https://doi.org/10.1016/  
j.isci.2024.110585](https://doi.org/10.1016/j.isci.2024.110585)



## Article

Reiterated male-to-female violence disrupts hippocampal estrogen receptor  $\beta$  expression, prompting anxiety-like behavior

Jacopo Agrimi,<sup>1,2</sup> Lucia Bernardele,<sup>1</sup> Naeem Sbaiti,<sup>2</sup> Marco Brondi,<sup>9</sup> Donato D'Angelo,<sup>1</sup> Marta Canato,<sup>1</sup> Ivan Marchionni,<sup>1</sup> Christian U. Oeing,<sup>3</sup> Giusy Barbara,<sup>4,5</sup> Beatrice Vignoli,<sup>6</sup> Marco Canossa,<sup>7</sup> Nina Kaludercic,<sup>1</sup> Gaya Spolverato,<sup>8</sup> Anna Raffaello,<sup>1</sup> Claudia Lodovichi,<sup>9,10,11</sup> Marco Dal Maschio,<sup>1,11,12,\*</sup> and Nazareno Paolucci<sup>1,2,12,13,\*</sup>

## SUMMARY

**Intimate partner violence (IPV) is a significant public health concern whose neurological/behavioral sequelae remain to be mechanistically explained. Using a mouse model recapitulating an IPV scenario, we evaluated the female brain neuroendocrine alterations produced by a reiterated male-to-female violent interaction (RMFVI). RMFVI prompted anxiety-like behavior in female mice whose hippocampus displayed a marked neuronal loss and hampered neurogenesis, namely reduced BrdU-DCX-positive nuclei and diminished dendritic arborization in the dentate gyrus (DG): effects paralleled by a substantial downregulation of the estrogen receptor  $\beta$  (ER $\beta$ ). After RMFVI, the DG harbored reduced brain-derived neurotrophic factor (BDNF) pools and tyrosine kinase receptor B (TrkB) phosphorylation. Accordingly, ER $\beta$  knockout (KO) mice had heightened anxiety and curtailed BDNF levels at baseline while dying prematurely during the RMFVI procedure. Strikingly, injecting an ER $\beta$  antagonist or agonist into the wild-type (WT) female hippocampus enhanced or reduced anxiety, respectively. Thus, reiterated male-to-female violence jeopardizes hippocampal homeostasis, perturbing the ER $\beta$ /BDNF axis and ultimately instigating anxiety and chronic stress.**

## INTRODUCTION

"Intimate partner violence" (IPV) is the physical/sexual violence, stalking, or psychological injury perpetrated by a current or former partner/spouse.<sup>1</sup> In 2022, the EU Agency for Fundamental Rights randomly performed interviews among the 28 countries of the UNION, with 42,002 women aged 18–74, 51.7% of whom reported being victims of IPV in their lifetime.<sup>2</sup> IPV can endanger the function of multiple organs and has an undeniable and appalling feature: the victims are primarily women.<sup>3</sup> On the heels of this evidence, getting a deeper grasp of the pathophysiological IPV sequelae becomes increasingly pressing.

IPV neurological and psychiatric repercussions have monopolized the lens of scientists and caregivers, especially epidemiologically.<sup>2</sup> Yet how IPV ignites/exacerbates brain/behavioral disorders, especially when reiterated, remains to be deciphered in full. Experimental models mimicking human IPV's critical features are crucial to addressing this unknown. To fill this gap, we adapted a recently validated animal model that leads a female mouse to social defeat,<sup>4</sup> amplifying the violent and prolonged interaction with an aggressive male (reiterated male-to-female violent interaction, RMFVI). Using fertile female mice, we tested whether RMFVI downregulates estrogen-mediated signaling, focusing on the hippocampus, a primary hub of mood control and a well-documented target of acute/chronic stress of different etiology.<sup>5</sup> Within it, we zoomed on the dentate gyrus (DG), a prominent neurogenesis site in the adult brain.<sup>6</sup> More in detail, we tested whether, at the

<sup>1</sup>Department of Biomedical Sciences, University of Padova, Padova, Italy

<sup>2</sup>Department of Medicine, Johns Hopkins University School of Medicine, Baltimore, MD, USA

<sup>3</sup>Department of Internal Medicine and Cardiology, Charité University Medicine, Berlin, Germany

<sup>4</sup>Service for Sexual and Domestic Violence, Fondazione IRCCS, Ospedale Maggiore Policlinico, Milan, Italy

<sup>5</sup>Department of Clinical Science and Community Health, University of Milan, Milan, Italy

<sup>6</sup>Department of Physics, University of Trento, 38123 Trento, Italy

<sup>7</sup>Department of Cellular, Computational, and Integrative Biology, University of Trento, Trento, Italy

<sup>8</sup>Department of Surgical Oncological and Gastrointestinal Sciences, University of Padova, Padova, Italy

<sup>9</sup>Neuroscience Institute -CNR, Padova, Italy

<sup>10</sup>Veneto Institute of Molecular Medicine, Padova, Italy

<sup>11</sup>Padova Neuroscience Center, Padova, Italy

<sup>12</sup>These authors contributed equally

<sup>13</sup>Lead contact

\*Correspondence: marco.dalmaschio@unipd.it (M.D.M.), npaoloc1@jhm.edu (N.P.)

<https://doi.org/10.1016/j.isci.2024.110585>



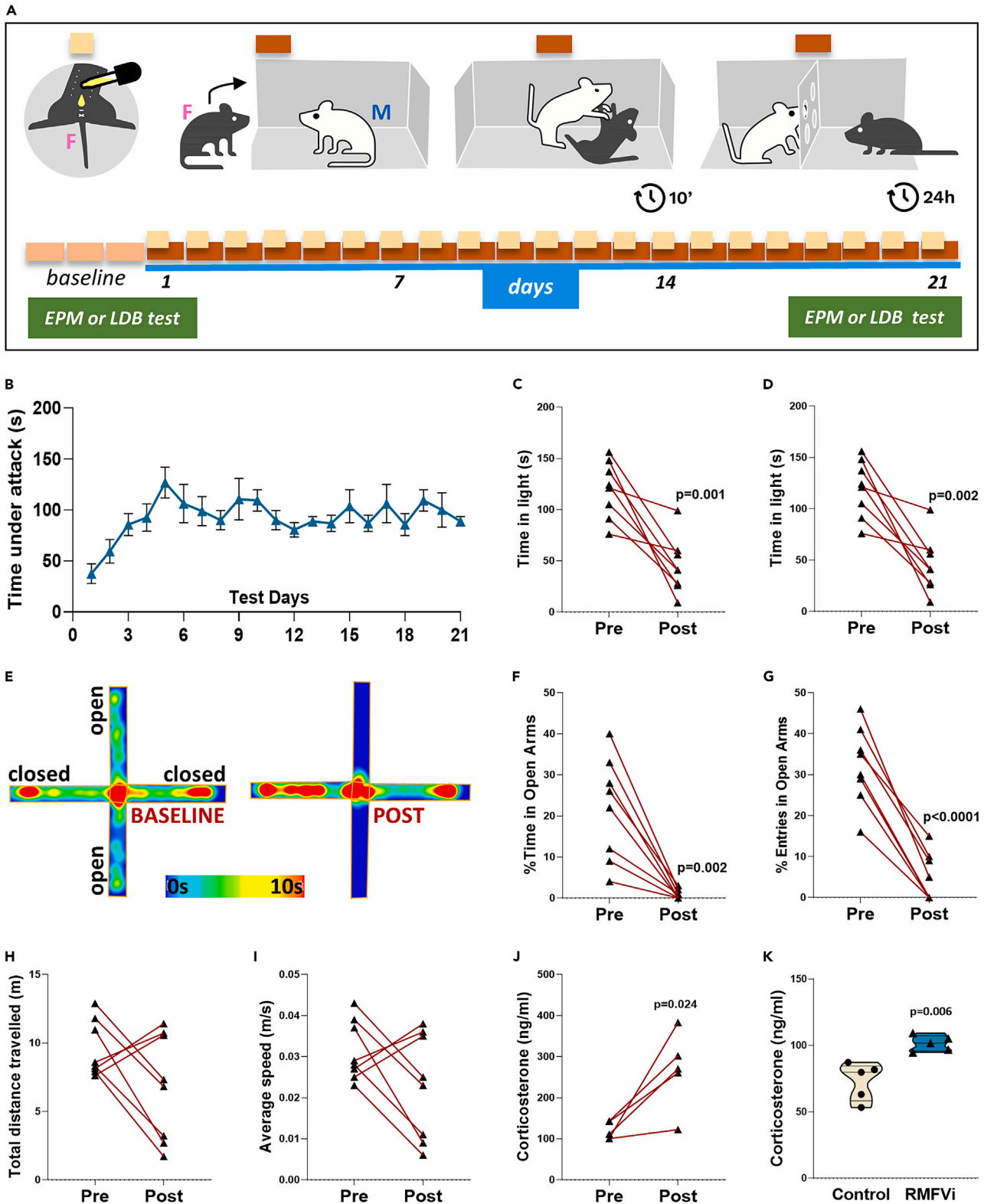


**Figure 1. RMFVi induces anxiety-like behavior**

(A) Reiterated male-to-female violent interaction (RMFVi), explicative scheme.  
(B) Daily time under males attack spent by the females during RMFVi procedure.

**Figure 1. Continued**

(C and D) Light-dark box test (LDB), (C) number of transitions from the dark to the light compartment, RMFVI vs. control,  $n = 8$ ,  $p < 0.0001$  (paired t-test), (D) time spent by mice in the light compartment, RMFVI vs. control,  $n = 8$ ,  $p < 0.0001$  (paired t-test).

(E–I) Elevated plus maze test (EPM), (E) heat plot of time spent in different parts of the maze at baseline (left) and after RMFVI (right), (F) percentage of entries in the open arms, pre-RMFVI vs. 21 days RMFVI,  $n = 8$ ,  $p < 0.0001$  (paired t-test), (G) percentage of time spent in the open arms, pre-RMFVI vs. 21 days RMFVI,  $n = 8$ ,  $p = 0.002$  (paired t-test), (H) total distance traveled by the animals, pre-RMFVI vs. 21 days RMFVI,  $n = 8$  and (I) average speed of the animal movements, pre-RMFVI vs. 21 days RMFVI,  $n = 8$ .

(J) Circulating corticosterone, pre-RMFVI vs. 21 days RMFVI,  $n = 5$ ,  $p = 0.024$  (Wilcoxon signed rank test).

(K) Central corticosterone, pre-RMFVI vs. 21 days RMFVI,  $n = 5$ ,  $p = 0.006$  (Mann-Whitney U test).

hippocampal/DG level, RMFVI alters estrogen receptor (ER) expression patterns and dependent pro-survival extracellular signal-regulated kinase (ERK) signaling that, in turn, controls the expression of BDNF.<sup>7</sup> BDNF is essential for proper neuronal development and response to stress conditions of different etiology in adulthood.<sup>8</sup> We grounded our hypothesis on evidence showing that ER $\beta$  selective agonists, particularly, exert potent anxiolytic effects during animal behavioral testing by inhibiting the adrenocorticotrophic hormone (ACTH) and corticosterone response to stress.<sup>9</sup> Moreover, estrogen can shape BDNF expression in many ways. First, by convergence, when interacting with BDNF receptors, namely TrkB; estrogen and BDNF/TrkB activate transcription factors, such as cAMP response element-binding protein (CREB), leading to the transcription of a series of pro-survival genes, including *bdnf* itself.<sup>7</sup> Second, by induction. Indeed, *bdnf* contains a canonical estrogen response element, and estrogen can also directly modify the *bdnf* promoter epigenetically.<sup>7</sup>

**RESULTS****RMFVI triggers anxiety-like behavior in female mice**

We tailored a recently validated social defeat protocol in female mice<sup>4</sup> derived from the resident-intruder paradigm. The latter is widely used to investigate human psychosocial stress through animal models.<sup>10</sup> However, we extended the time of violent interaction from 10 to 21 days to better follow the trajectory of the neurogenic process.<sup>11</sup> In doing so, we were able to create a setting of chronic physical and psychological violence in a male vs. female mouse context (Figure 1A) long enough to monitor possible RMFVI-triggered alterations of the neurogenic process in the female ones. Consistently, the RMFVI procedure led to daily physical male-toward-female attacks (computed in  $\cong 100$  s per day) (Figure 1B) while mixing this physical, aggressive behavior with a sensorial intimation on a recurrent basis. Following 21 days of this challenge, we set out to determine whether the planned RMFVI procedure was sufficient to perturb the female mouse's behavior, focusing on exploratory activity and anxiety. Therefore, at the end of the procedure, the female mice were subjected to behavioral tests, including the light-dark box (LDB) and the elevated plus maze (EPM).<sup>12</sup> For the LDB test, we compared RMFVI-exposed female mice's behavior with their baseline performance (RMFVI). The two main parameters of the LDB test revealed a significant surge of anxiety-like behavior coupled with reduced exploratory activity in female mice exposed to RMFVI. More in detail, they spent significantly less time in the light compartment (Figure 1C,  $p = 0.001$ ) and transitioned less to the light one (Figure 1D,  $p = 0.002$ ). To exclude a possible bias due to having repeated the same test (twice) in the same group of animals, we evaluated a cross-sectional scheme employing two additional groups: (1) female mice subjected to the LDB test only at the end of the RMFVI procedure and (2) control age-matched females not exposed to the RMFVI paradigm. As shown in Figure S2, LDB performed longitudinally led to outcomes comparable to those obtained with the cross-sectional modality (time in light, results from the longitudinal study: pre-RMFVI  $120 \text{ s} \pm 28 \text{ s}$  vs. post-RMFVI  $45 \text{ s} \pm 27 \text{ s}$ ; time in light, results from the cross-sectional study: control  $111 \text{ s} \pm 21 \text{ s}$  vs. RMFVI  $46 \text{ s} \pm 26 \text{ s}$ ). For the EPM test, we compared RMFVI-exposed female mice's behavior with their baseline performance. EPM test confirmed and strengthened the LDB outcomes. Indeed, after RMFVI, the percentage of time spent in the maze open arms plummeted to almost zero ( $\cong 95\%$  drop,  $p = 0.002$ ; Figure 1F). The same was evident for the percentage of entries in the open arms (pre vs. post =  $-90\%$ ,  $p < 0.0001$ , Figure 1G). Yet, locomotor activity was unaffected in these mice. Indeed, the total distance traveled by the female mice and average speed were unchanged after RMFVI (Figures 1H and 1I). Finally, we measured the circulating and central corticosterone levels, a marker widely used in stress paradigms,<sup>13</sup> finding a significant increase after 21 days of RMFVI ( $p = 0.024$  and  $p = 0.006$ , Figures 1J and 1K). Thus, the RMFVI paradigm engendered a forthright anxiety-like behavior framed into a persistent general stress context, all typical features of human IPV.

**RMFVI triggers apoptosis and halts neurogenesis at the hippocampal DG level**

The hippocampus, particularly the DG, is a primary hub for mood control, memory consolidation, and spatial exploration.<sup>5,14,15</sup> Of relevance, alterations at this level are manifest in experimental and human forms of acute or chronic stress.<sup>6,16,17</sup> Yet, no studies have evaluated the impact of reiterated IPV-like conditions on the hippocampus, specifically the DG. To fill this gap, we first assessed the amount of apoptosis as a primary marker of cell damage. TUNEL assay revealed that cell death extent in the DG doubled after RMFVI, as indicated by the increased number of TUNEL-positive nuclei spread throughout this structure, i.e., in the granular, subgranular, and hilus zones (Figures 2B and 2C) (control vs. RMFVI;  $p = 0.008$ ). Next, we quantified adult hippocampal neurogenesis, combining BrdU labeling of *de novo* DNA synthesizing cells with doublecortin (DCX) staining, a protein associated with neuronal differentiation and functionally linked to cell migration.<sup>18</sup> To this end, we injected BrdU intraperitoneally to control (i.e., no RMFVI entering) mice and those randomized to undergo the full RMFVI protocol. After 21 days of RMFVI, the number of BrdU+ cells, colocalized with DCX+ cells, was markedly diminished in the DG (Figures 2D and 2E; control vs. RMFVI,  $p = 0.008$ ). DCX is only expressed in cells contributing to adult neurogenesis in the DG, and previous studies<sup>19</sup> show that DCX+ cells

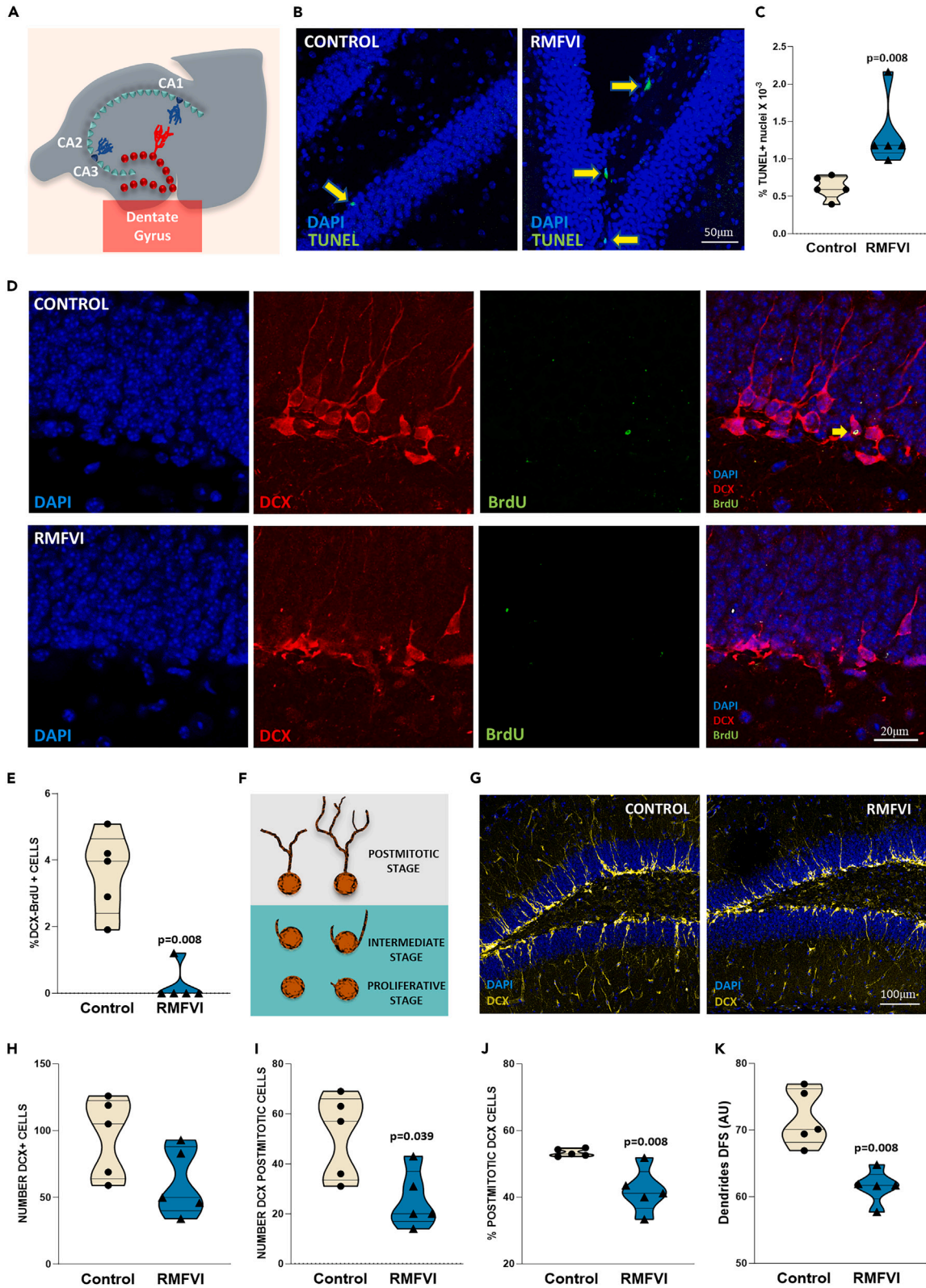


**Figure 2. RMFVI triggers apoptosis while impairing neurogenesis in the DG**

- (A) Scheme of the hippocampal formation morphology redrawn from Toda T. et al.<sup>20</sup>
- (B) Representative images of IF with TUNEL assay in the DG of controls and RMFVI-inflicted mice.
- (C) TUNEL positive nuclei quantification, control vs. RMFVI,  $n = 5$ ,  $p = 0.08$  (Mann-Whitney U test).
- (D) Representative images of IF staining for DAPI, BrdU, and DCX in the DG of controls and RMFVI-inflicted mice.
- (E) BrdU/DCX positive cells quantification, control vs. RMFVI,  $n = 5$ ,  $p = 0.08$  (Mann-Whitney U test).
- (F) Representative scheme of DCX positive cell differentiation.
- (G) Representative images of IF staining for DAPI and DCX in the DG of controls and RMFVI-inflicted mice.
- (H) DCX positive cells quantification, control vs. RMFVI,  $n = 5$ .
- (I) DCX positive cells (classified as postmitotic) quantification, control vs. RMFVI,  $n = 5$ ,  $p = 0.039$  (Mann-Whitney U test).
- (J) Percentage of DCX postmitotic positive cells (on total DCX positive cells), control vs. RMFVI,  $n = 5$ ,  $p = 0.008$  (Mann-Whitney U test).
- (K) Average dendrite length of DCX postmitotic positive cells, control vs. RMFVI,  $n = 5$ ,  $p = 0.008$  (Mann-Whitney U test).

can be subtyped according to the neurogenic process stage, from immature through proliferative to postmitotic (Figure 2F). Hence, we next analyzed the number and percentage of DCX+ cells in the postmitotic phase.<sup>19</sup> We found markedly lower DCX+ postmitotic cells in the DG of RMFVI-inflicted subjects than controls (Figures 2G–2J,  $p = 0.039$ ,  $p = 0.008$ ). When assessing the distance from the soma of the DCX dendrites as an index of arborization and differentiation, we found it sizably reduced in the RMFVI group (Figure 2K,  $p = 0.008$ ). These data reveal that the RMFVI paradigm can induce cell death and impair the neurogenic process in the hippocampal DG.

**RMFVI impairs ER $\beta$  expression in the hippocampus/DG of female mice**

Estrogens are involved in the brain's sexual differentiation and several neuronal events, such as survival and synaptic plasticity.<sup>21,22</sup> Moreover, estradiol (E2) governs mood balance and pain regulation, mainly through its specific receptors ER $\alpha$  and ER $\beta$ .<sup>23</sup> Previous studies have extensively evaluated the repercussions of violent aggression perpetrated by a male mouse toward a female one.<sup>4</sup> However, to our knowledge, whether estrogens and their receptors are affected by a social stress-related paradigm is currently unclear. Of note, the protective role exerted by estrogen and ER $\beta$ -dependent signaling, in particular, on the hippocampal structure and function, has been repeatedly reported (as reviewed in a study by Bean et al.<sup>24</sup>). Against this background, we first measured the circulating and whole-brain levels of E2 before and after RMFVI. We found that, after it, both systemic and central E2 levels were above pre-RMFVI values (Figures 3A and 3B). To extend this picture, we investigated ER $\alpha$  and ER $\beta$ 's expression levels. In small and large mammals, ER $\alpha$  and ER $\beta$  are expressed ubiquitously in the brain. Yet, ER $\beta$  expression is particularly prominent in the hippocampus, especially in the DG<sup>25</sup> (Figure 3C). We observed a substantial drop in the ER $\beta$  expression and unchanged levels of ER $\alpha$  at the hippocampal level (Figures 3D–3F). When zooming on the DG via IF, we noted a 70% decline in the ER $\beta$  expression in RMFVI female mice ( $p < 0.0001$ , Figures 3G and 3H). We interpret these data to indicate that RMFVI hinders ER $\beta$  expression while increasing circulating E2 content.

**RMFVI downsizes the BDNF/TrkB axis in the DG**

In the brain, ER $\beta$  stimulation can lead to ERK phosphorylation,<sup>26</sup> inducing BDNF expression and, thus, protective cues in the target organs/cells.<sup>7,27</sup> The same occurs with TrkB agonism in the brain<sup>28</sup> and the heart, as recently shown by us.<sup>29</sup> On these grounds, we next determined whether a lack of ER $\beta$  and/or TrkB signaling is coupled to a reduced ERK activation, i.e., phosphorylation, leading, in turn, to BDNF depletion in the hippocampus. Consistent with our hypothesis, RMFVI markedly dropped ERK phosphorylation levels in the hippocampal DG ( $p = 0.0025$ ; Figures 4A and 4B). Next, we tested whether these events prompted local impoverishment of hippocampal/DG BDNF pools. When examining them in the whole brain via ELISA, we first found no significant differences between control and RMFVI-inflicted females (Figure S4A). However, when zooming on the hippocampus, we noticed a marked BDNF depletion (Figure S4B,  $p = 0.031$ ). Consistent with the aforementioned-reported findings, this decline was even more pronounced in the DG (–70%, Figures 4C and 4D,  $p = 0.008$ ). In unison, we also detected a significant decrease in TrkB phosphorylation (Figures 4E and 4F,  $p = 0.0079$ ) in RMFVI-inflicted mice. Thus, RMFVI depletes hippocampal BDNF pools, especially in the DG. We can ascribe this decline to a lack of ER $\beta$ /ERK and/or TrkB agonistic signaling, on the one hand, and/or enhanced suppressive action exerted by chronic glucocorticoid receptor (GR) activation, on the other.

**Downregulating ER $\beta$  signaling resembles RMFVI-ignited behavioral and molecular signatures**

To cement the view that ER $\beta$  is involved in the aforementioned post-RMFVI behavioral and humoral alterations, we extended our studies to ER $\beta$  KO mice, evaluating them at baseline and after RMFVI. At baseline, ER $\beta$  KO mice already displayed a constitutive anxiety-like behavior, as evidenced by the EPM test's main parameters, characterized by a significant decrease in time and percentage of entries in the open arms of the maze (Figures 5A and 5B). We then subjected wild-type (WT) and ER $\beta$  KO mice to the full RMFVI protocol, evaluating survival via the Kaplan-Meier curves. All WT mice survived the entire RMFVI procedure. Conversely, four out of nine ER $\beta$  KO mice did not survive until the end of the protocol ( $p = 0.038$ , Figure 5C). The E2 circulating levels rose significantly after RMFVI in WT mice, as shown in Figure 3A and confirmed in Figure 5D. Conversely, ER $\beta$  KO mice already had substantially higher systemic E2 at baseline than WT. In the former, RMFVI still heightened E2 circulating levels, which did not outweigh those found in post-RMFVI WT mice (Figure 5D). In unison, ER $\beta$  KO displayed a drastic decline in BDNF expression, at the DG level, already at baseline, as compared to age-matched WT counterparts (IF in Figures 5E and 5F). Of note, after RMFVI, BDNF expression was markedly reduced in WT mice and did not drop further in the ER $\beta$  KO mice

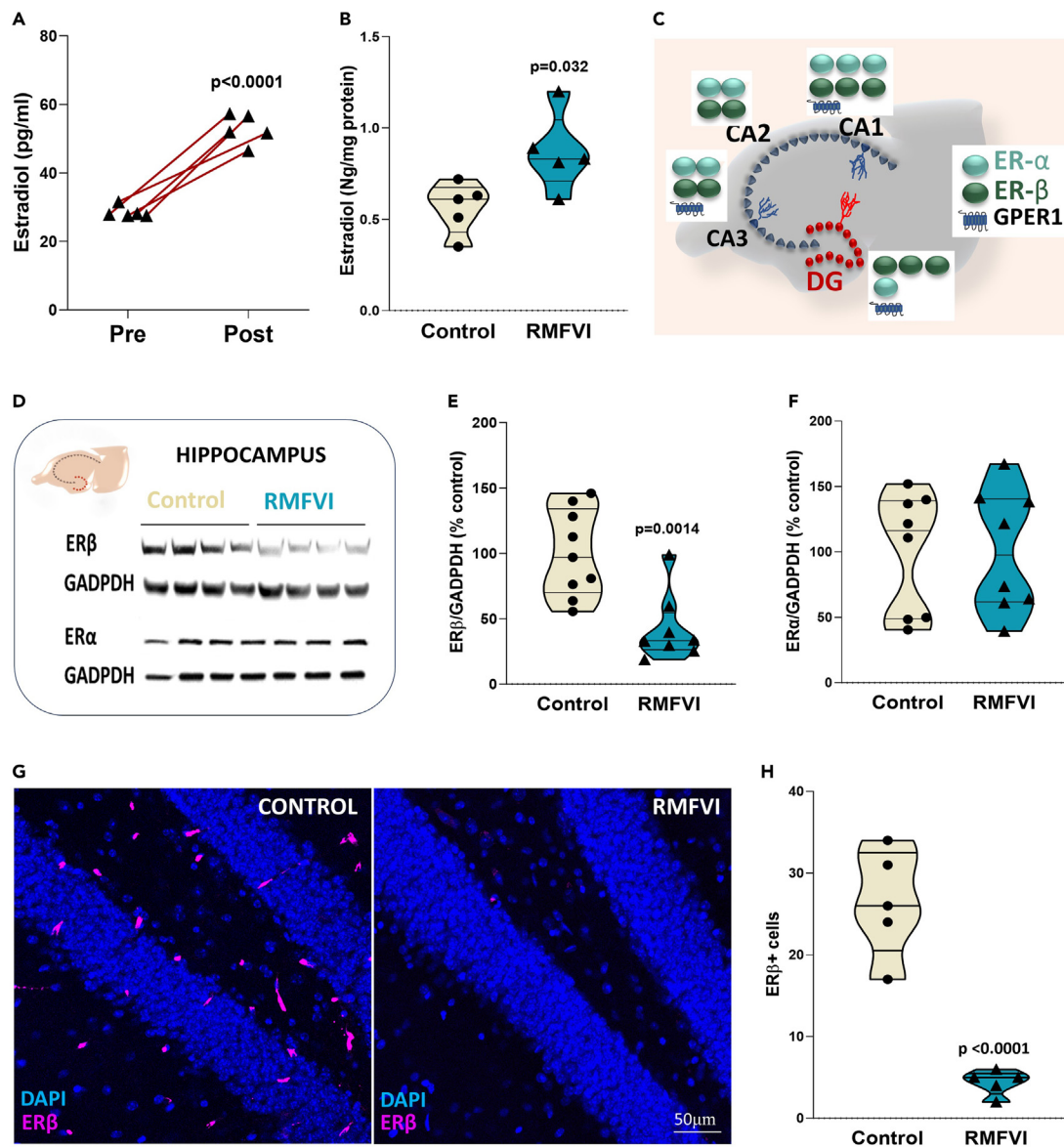


**Figure 3. RMFVI jeopardizes ER $\beta$  expression in the female hippocampus**

(A) Circulating 17-beta-estradiol measured by ELISA at baseline and after 21 days of RMFVI,  $n = 5$ ,  $p < 0.0001$  (Wilcoxon signed rank test).  
 (B) 17-beta-estradiol measured by ELISA in lysates of whole brain from controls and RMFVI-exacted mice,  $n = 5$ ,  $p = 0.022$  (Mann-Whitney U test).  
 (C) Scheme of estrogen receptor expression in different hippocampal areas.  
 (D–F) Western blot for ER $\alpha$  and ER $\beta$  in the hippocampus of controls and RMFVI-imposed mice, (D) representative immunoblotting in the hippocampus for ER $\alpha$ , ER $\beta$ , and GAPDH; (E) quantification of ER $\beta$  (normalized to GAPDH content), control vs. RMFVI,  $n = 8$ ,  $p = 0.0014$  (unpaired t-test); (F) quantification of ER $\alpha$  (normalized to GAPDH content), control vs. RMFVI,  $n = 8$ .  
 (G) Representative images of IF staining for ER $\beta$  in the DG, control, and RMFVI-inflicted mouse.  
 (H) Quantification of IF staining for ER $\beta$  in the DG, control vs. RMFVI,  $n = 5$ ,  $p < 0.0001$  (Mann-Whitney U test).

(Figures 5E and 5F). Finally, to causally bond the RMFVI behavioral outcomes to a hippocampal-driven molecular mechanism involving the ER $\beta$ -pathway, we resorted to a targeted bidirectional manipulation of the ER $\beta$  activity. We precisely silenced or enhanced ER $\beta$  receptor activity in the hippocampus, using stereotaxic injections of either an ER $\beta$  antagonist (4-[2-Phenyl-5,7-bis(trifluoromethyl)pyrazolo[1,5-a]pyrimidin-3-yl]phenol, PHTPP), or an agonist (diarylpropionitrile, DPN) in female mice. An image from staining with trypan blue for targeting accuracy is shown in Figure 5G. After complete recovery, we evaluated the exploratory behavior of WT female mice via the LDB test. Consistently with our initial hypothesis and garnered RMFVI evidence, we found that the injection of the ER $\beta$  antagonist markedly increased anxiety-like behavior and abated the exploratory activity of the female mice compared to the saline-injected ones, as revealed by the drastic reduction in

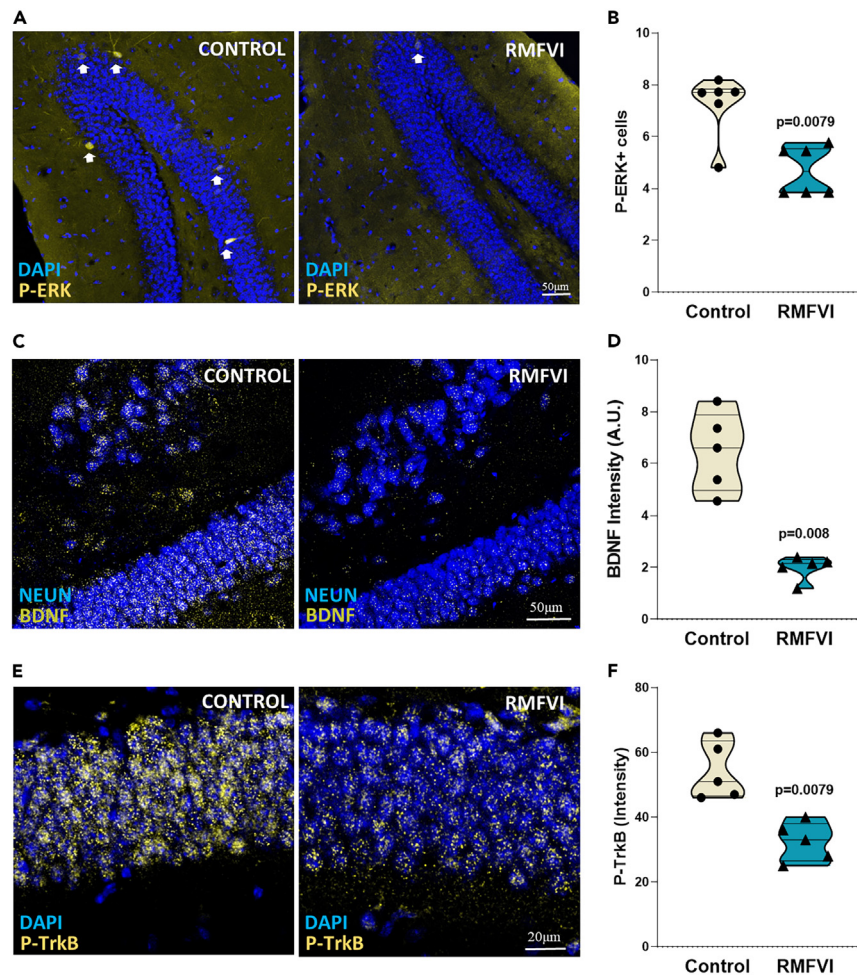


**Figure 4. RMFVI alters BDNF/TrkB signaling in the DG**

(A) Representative images of IF staining for P-ERK in the DG, control, and RMFVI mice.  
 (B) Quantification of IF staining for P-ERK+ cells in the DG, control vs. RMFVI,  $n = 5$ ,  $p = 0.0079$  (Mann-Whitney U test).  
 (C) Representative images of IF staining for BDNF in the DG, control, and RMFVI-inflicted mice.  
 (D) Quantification of IF staining for BDNF in the DG, control vs. RMFVI,  $n = 5$ ,  $p = 0.008$  (Mann-Whitney U test).  
 (E) Representative images of IF staining for P-TrkB in the DG, control, and RMFVI mice.  
 (F) Quantification of IF staining for P-TrkB in the DG, control vs. RMFVI,  $n = 5$ ,  $p = 0.0079$  (Mann-Whitney U test).

the time spent in light during the test ( $p = 0.013$ , Figure 5H) and the number of transitions to the light compartment ( $p = 0.033$ , Figure 5I). Conversely, the injection of the ER $\beta$  agonist resulted in an orthogonal behavior: the time spent in light by the female mice increased significantly compared to controls ( $p = 0.045$ , Figure 5H). This dataset demonstrates that, in WT female mice, pharmacological interventions apt to modify ER $\beta$  activation, thus dependent signaling, at the hippocampal level, are penetrant enough to trigger sizable behavioral changes in the anxiety domain, as revealed here by the LDB test.

## DISCUSSION

The main findings of our study, conducted in a mouse model of reiterated male-to-female violent interaction, are that such violent interaction (1) propels anxiety-like behavior in female mice; (2) fuels apoptosis and impairs neurogenesis at the hippocampal level; and (3) jeopardizes ER $\beta$  expression, increasing local and circulating stress hormones, while downsizing the prosurvival-enhancing properties of BDNF/TrkB signaling in the hippocampus.

We have adopted and modified a method for mimicking some prominent features of human IPV, such as reiterated male-to-female physical and psychological violence. We focused on the hippocampus, especially the DG, given its vulnerability to social stress conditions,<sup>13,14</sup> and its prominent ERs expression.<sup>25</sup>



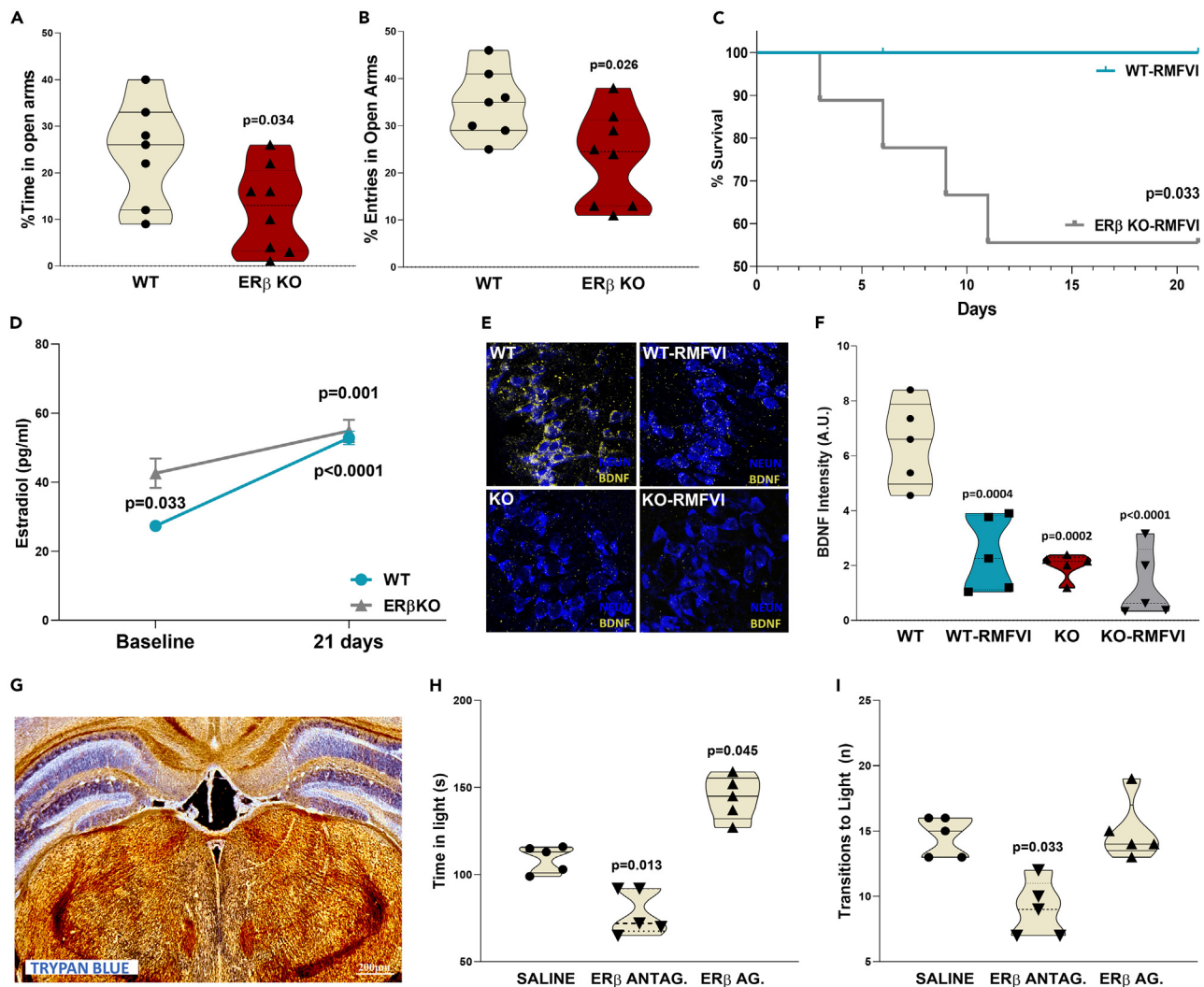


**Figure 5. Manipulation of ER $\beta$  signaling reproduces RMFVI-ignited behavioral perturbations and estradiol and BDNF decline**

(A and B) Elevated plus maze test for WT and ER $\beta$  KO, (A) percentage of time spent in the open arms from WT and ER $\beta$  KO mice,  $n = 8$ ,  $p = 0.034$  (unpaired t-test) (B) percentage of entries in the open arms from WT and ER $\beta$  KO mice,  $n = 8$ ,  $p = 0.026$  (unpaired t-test).

(C) Survival Kaplan-Meier curves of WT and ER $\beta$  KO mice during RMFVI procedure,  $n = 9$ ,  $p = 0.023$ .

(D) Circulating 17-beta-estradiol measured by ELISA at baseline and after 21 days RMFVI in WT and ER $\beta$  KO mice,  $n = 5$ , baseline WT vs. baseline ER $\beta$  KO mice  $p = 0.033$ , WT baseline vs. 21 days RMFVI,  $p < 0.0001$ , ER $\beta$  KO mice baseline vs. 21 days RMFVI,  $p = 0.001$  (Friedman's test).

(E) Representative images of IF staining for BDNF in the DG (hilar cells), WT, and ER $\beta$  KO mice before and after RMFVI.

(F) Quantification of IF staining for BDNF in the DG, control WT vs. ER $\beta$  KO mice, before and after RMFVI,  $n = 5$ ; WT vs. WT-RMFVI,  $p = 0.0004$ , WT vs. KO,  $p = 0.0002$ , WT vs. KO-RMFVI  $p < 0.0001$  (Kruskal-Wallis one-way test).

(G) Stereotaxic injection in the hippocampal formation: site of injection stained with trypan blue.

(H) Light-dark box test, time spent by mice in the light compartment,  $n = 5$ ; saline vs. PHTPP (antagonist),  $p = 0.013$ ; Saline vs. DPN (agonist),  $p = 0.045$  (Kruskal-Wallis one-way test).

(I) Light-dark box test, transition to the light compartment,  $n = 5$ ; saline vs. PHTPP (antagonist),  $p = 0.033$  (Kruskal-Wallis one-way test).

After continuing physical attacks/sensorial intimidation by an aggressive male mouse, female mice develop anxiety-like behavior and chronic stress, two main features of human IPV. Of note, to exclude a possible bias due to having repeated the same test (twice) in the same group of animals, we studied two additional (separate) groups: (1) female mice subjected to the LDB test only at the end of the RMFVI procedure and (2) control age-matched females not exposed to the RMFVI paradigm and subjected to the LDB (cross-sectional studies). LDB performed longitudinally led to outcomes superimposable to those obtained with the cross-sectional modality (Figure S2). Indeed, the time in light spent by female mice pre-RMFVI was  $120 \text{ s} \pm 28 \text{ s}$  vs. post-RMFVI  $45 \text{ s} \pm 27 \text{ s}$  (longitudinal modality). These results dovetail nicely with those obtained with the cross-sectional approach:  $111 \text{ s} \pm 21 \text{ s}$  (control) vs.  $46 \text{ s} \pm 26 \text{ s}$  (post-RMFVI).

Estrogen plays a primary role in female subjects in response to chronic stress.<sup>30–32</sup> The current evidence—gathered with the stereotactic injection of an ER $\beta$  agonist or antagonist into the hippocampus—nicely cements this view, and further validates our initial hypothesis. At the same time, the premature death of ER $\beta$  KO mice during RMFVI could serve as an “extremization” of the central role ER $\beta$  signaling plays in RMFVI. Therefore, although not the sole mechanism at play, our data indicate male violence curtails ER $\beta$  receptor density in the female’s hippocampus, particularly in the DG. At this level, the lack of this protective signaling prompts neuronal cell death, deficient dendritic arborization, and impaired neurogenesis. This adverse remodeling owes, at least in part, to the defective estrogen-evoked activation of master regulators of cell behavior, such as ERK and its dependent prosurvival signaling, including, but not limited to, BDNF expression. Of note, in humans and other species, the link between hippocampal homeostasis (essential for mood regulation, stress response, memory, and spatial orientation) has been primarily studied in the context of psychopathology and aging in males.<sup>33,34</sup> Here, we extend it to reiterated physical violence suffered by the female at the hands of a male conspecific.

The involvement of the other ER isoforms, namely ER $\alpha$  and G protein-coupled estrogen receptor 1, in RMFVI hippocampal pathophysiology warrants further investigation. Notwithstanding, our data suggest a primary involvement of the ER $\beta$  isoform, which is also the most expressed in this brain area,<sup>25</sup> fitting nicely with consolidated evidence that ER $\alpha$  and ER $\beta$  exert opposing actions during stress responses.<sup>35</sup> Accordingly, Krezel and colleagues reported a heightened anxiogenic behavior in ER $\beta$  KO but not ER $\alpha$  KO mice.<sup>36</sup> Equally relevant, treatment with the highly potent ER $\beta$  agonist DPN increases the time spent in the open arms, in the EPM test, compared to vehicle-treated control animals.<sup>37</sup> While validating this notion, our current data also provide unprecedented evidence that stress conditions, such as RMFVI infliction, directly hinder ER $\beta$  density. In our model, the elevated (and likely compensatory) systemic E2 levels can favor binding with the  $\alpha$  isoform, whose expression, at least at the hippocampal level, remains unchanged, paradoxically exerting a negative effect on the pathways governed by the  $\beta$  isoform. However, as an alternative or additive mechanistic route underscoring ER $\beta$  downregulation, we could also entertain the methylation of the ER $\beta$  promoter (5’ untranslated region), increasingly recognized as a primary modality for regulating this ER isoform extent.<sup>38</sup> From a behavioral point of view, ER $\beta$  modulation is critical for serotonin and dopamine neurotransmission.<sup>39</sup> Thus, the current lack of ER $\beta$  stimulation fuels the anxiety-like behavior found in RMFVI-inflicted WT mice and is exacerbated in ER $\beta$  KO ones.

At the hippocampal level, estrogen, corticosteroids, and BDNF influence each other levels,<sup>40,41</sup> hence the adaptative response to stress conditions.<sup>42</sup> Under the current scenario, we speculate that lack of ER $\beta$ , therefore unopposed corticosteroid receptor stimulation, contributes to the overall hippocampal structural and functional impairment by affecting, among other effects, TrkB activation status. The present evidence of a reduced extent of TrkB phosphorylation after RMFVI grants support to this contention. Another possible reason accounting for the loss of hippocampal BDNF in RMFVI female mice is that elevated levels of corticosteroids, via GR activation, suppress neuronal BDNF expression through direct binding to the *bdnf* regulatory sequence.<sup>42</sup> We can envision future, in-depth studies employing *in vivo* imaging and electrophysiology approaches to more longitudinally track down hippocampal and brain dynamic perturbations. Nevertheless, our intent here was to provide an initial mechanistic template, i.e., RMFVI disruption of the ER $\beta$ /BDNF axis, on which to mold additional evaluations of other brain regions equally relevant for behavioral homeostasis, such as the frontal cortices, insula, amygdala, and hypothalamus.

Our study demonstrates that recurrent physical/sensorial violence directly impacts the female hippocampus, accounting for primary shifts in behavioral control, such as the onset/maintenance of anxiety and chronic stress. At the same time, from a therapeutic perspective, our current data suggest that, in IPV victims, preserving ER $\beta$  integrity should be at the core of the therapeutic attempts. This proposition has additional significant clinical implications. Indeed, if generalized, the loss of ER $\beta$  signaling could favor the progression of many forms of cancer in women. Unfortunately, cancer diagnoses are increasing in IPV-victimized women.<sup>43</sup> Moreover, studies suggest ER $\beta$  activation may be a promising avenue for reducing menopause-related hot flashes and memory dysfunction and also to lessen the risk of neurodegenerative disorders, such as Alzheimer’s disease.<sup>44</sup>

Women victims of IPV show a plethora of pathological signs and symptoms spread throughout almost all body areas. Often, these conditions are treated separately and symptomatically. By grouping them in one common pathogenic mechanism, i.e., disrupted ER $\beta$ /BDNF signaling, we offer new potential therapeutic avenues, such as selective ER $\beta$  agonists derived from natural compounds,<sup>45,46</sup> to taper off the acute and chronic central repercussions of reiterated IPV.

### Limitations of the study

Our study has some limitations. First, additional future experiments involving daily administration of the ER $\beta$  agonist, DPN, to RMFVI-subjected mice should determine whether targeting ER $\beta$  signaling would mitigate the acute (or long-term) effects of chronic stress inflicted by males on females. The same is true for selective TrkB agonists. Second, looking at the GR activity in RMFVI female mice deserves full consideration in future *ad hoc* dedicated studies. Finally, we did not evaluate other brain regions equally prominent for behavioral homeostasis, such as the frontal cortices, insula, amygdala, and hypothalamus.

### STAR★METHODS

Detailed methods are provided in the online version of this paper and include the following:

- KEY RESOURCES TABLE
- RESOURCE AVAILABILITY
  - Lead contact
  - Materials availability

- Data and code availability
- EXPERIMENTAL MODEL AND STUDY PARTICIPANT DETAILS
- METHOD DETAILS
  - Behavioral tests
- QUANTIFICATION AND STATISTICAL ANALYSIS

## SUPPLEMENTAL INFORMATION

Supplemental information can be found online at <https://doi.org/10.1016/j.isci.2024.110585>.

## ACKNOWLEDGMENTS

This study was funded by MSCA action (Marie Skłodowska-Curie Actions) PINK (to J.A.), EU VISGEN MSCA-RISE-2016, EU NEURAM FE-TOPEN-RIA-2014-2015 to (M.D.M), and NIH-NHLBI R01 HL136918 (to N.P.). Thanks to Dr. Anna Sanga for the digital scheme (Figure 1A).

## AUTHOR CONTRIBUTIONS

Literature search: J.A., M.D.M., N.P., and G.B. Study design: J.A., C.L., M.D.M., and N.P. Animal data collection: J.A., L.B., N.S., M.B., M.C., and I.M. Molecular and histological data collection: J.A., L.B., N.S., M.B., D.D'A., and MC. Data analysis: J.A., L.B., N.S., C.U.O., D.D'A., and N.P. Data interpretation: J.A., B.V., G.S., A.R., M.C., M.D.M., and N.P. Drafting of the manuscript: J.A. and N.P. Figures: J.A. and N.P. Critical manuscript revision: J.A., G.B., B.V., I.M., C.U.O., M.C., N.K., A.R., C.L., M.D.M., and N.P.

## DECLARATION OF INTERESTS

The authors declare no conflicts of interests.

Received: October 24, 2023

Revised: April 29, 2024

Accepted: July 23, 2024

Published: July 25, 2024

## REFERENCES

1. Miller, E., and McCaw, B. (2019). Intimate Partner Violence. *N. Engl. J. Med.* 380, 850–857. <https://doi.org/10.1056/NEJMra1807166>.
2. Barbier, A., Chariot, P., and Lefèvre, T. (2022). Intimate partner violence against ever-partnered women in Europe: Prevalence and associated factors—Results from the violence against women EU-wide survey. *Front. Public Health* 10, 1033465. <https://doi.org/10.3389/fpubh.2022.1033465>.
3. Oram, S., Fisher, H.L., Minnis, H., Seedat, S., Walby, S., Hegarty, K., Rouf, K., Angénioux, C., Callard, F., Chandra, P.S., et al. (2022). The Lancet Psychiatry Commission on intimate partner violence and mental health: advancing mental health services, research, and policy. *Lancet Psychiatr.* 9, 487–524. [https://doi.org/10.1016/S2215-0366\(22\)00008-6](https://doi.org/10.1016/S2215-0366(22)00008-6).
4. Harris, A.Z., Atsak, P., Bretton, Z.H., Holt, E.S., Alam, R., Morton, M.P., Abbas, A.I., Leonardo, E.D., Bolkan, S.S., Hen, R., and Gordon, J.A. (2018). A Novel Method for Chronic Social Defeat Stress in Female Mice. *Neuropsychopharmacology* 43, 1276–1283. <https://doi.org/10.1038/npp.2017.259>.
5. Anacker, C., and Hen, R. (2017). Adult hippocampal neurogenesis and cognitive flexibility — linking memory and mood. *Nat. Rev. Neurosci.* 18, 335–346. <https://doi.org/10.1038/nrn.2017.45>.
6. Anacker, C., Luna, V.M., Stevens, G.S., Millette, A., Shores, R., Jimenez, J.C., Chen, B., and Hen, R. (2018). Hippocampal neurogenesis confers stress resilience by inhibiting the ventral dentate gyrus. *Nature* 559, 98–102. <https://doi.org/10.1038/s41586-018-0262-4>.
7. Scharfman, H.E., and MacLusky, N.J. (2006). Estrogen and brain-derived neurotrophic factor (BDNF) in hippocampus: Complexity of steroid hormone-growth factor interactions in the adult CNS. *Front. Neuroendocrinol.* 27, 415–435. <https://doi.org/10.1016/j.yfrne.2006.09.004>.
8. Marosi, K., and Mattson, M.P. (2014). BDNF mediates adaptive brain and body responses to energetic challenges. *Trends Endocrinol. Metab.* 25, 89–98. <https://doi.org/10.1016/j.tem.2013.10.006>.
9. Weiser, M.J., Foradori, C.D., and Handa, R.J. (2008). Estrogen receptor beta in the brain: From form to function. *Brain Res. Rev.* 57, 309–320. <https://doi.org/10.1016/j.brainresrev.2007.05.013>.
10. Koolhaas, J.M., Coppens, C.M., de Boer, S.F., Buwalda, B., Meerlo, P., and Timmermans, P.J.A. (2013). The Resident-intruder Paradigm: A Standardized Test for Aggression, Violence and Social Stress. *JoVE* 4367, e4367. <https://doi.org/10.3791/4367>.
11. Bergami, M., Berninger, B., and Canossa, M. (2009). Conditional deletion of TrkB alters adult hippocampal neurogenesis and anxiety-related behavior: The relationship between visual long-term memory and change blindness. *Commun. Integr. Biol.* 2, 14–16. <https://doi.org/10.4161/cib.2.1.7349>.
12. Tucker, L.B., and McCabe, J.T. (2021). Measuring Anxiety-Like Behaviors in Rodent Models of Traumatic Brain Injury. *Front. Behav. Neurosci.* 15, 682935. <https://doi.org/10.3389/fnbeh.2021.682935>.
13. Joëls, M., Karst, H., and Sarabdjitsingh, R.A. (2018). The stressed brain of humans and rodents. *Acta Physiol.* 223, e13066. <https://doi.org/10.1111/apha.13066>.
14. Campbell, S., and Macqueen, G. (2004). The role of the hippocampus in the pathophysiology of major depression. *J. Psychiatry Neurosci.* 29, 417–426.
15. Moser, E.I., Moser, M.-B., and McNaughton, B.L. (2017). Spatial representation in the hippocampal formation: a history. *Nat. Neurosci.* 20, 1448–1464. <https://doi.org/10.1038/nn.4653>.
16. Agrimi, J., Spalletti, C., Baroni, C., Keceli, G., Zhu, G., Caragnano, A., Matteucci, M., Chelko, S., Ramirez-Correa, G.A., Bedja, D., et al. (2019). Obese mice exposed to psychosocial stress display cardiac and hippocampal dysfunction associated with local brain-derived neurotrophic factor depletion. *EBioMedicine* 47, 384–401. <https://doi.org/10.1016/j.ebiom.2019.08.042>.
17. Surget, A., and Belzung, C. (2022). Adult hippocampal neurogenesis shapes adaptation and improves stress response: a mechanistic and integrative perspective. *Mol. Psychiatry* 27, 403–421. <https://doi.org/10.1038/s41380-021-01136-8>.
18. Francis, F., Koulakoff, A., Boucher, D., Chafey, P., Schaar, B., Vinet, M.-C., Friocourt, G., McDonnell, N., Reiner, O., Kahn, A., et al. (1999). Doublecortin Is a Developmentally Regulated, Microtubule-Associated Protein Expressed in Migrating and Differentiating Neurons. *Neuron* 23, 247–256. [https://doi.org/10.1016/S0896-6273\(00\)80777-1](https://doi.org/10.1016/S0896-6273(00)80777-1).

19. Plümpe, T., Ehninger, D., Steiner, B., Klempin, F., Jessberger, S., Brandt, M., Römer, B., Rodriguez, G.R., Kronenberg, G., and Kempermann, G. (2006). Variability of doublecortin-associated dendrite maturation in adult hippocampal neurogenesis is independent of the regulation of precursor cell proliferation. *BMC Neurosci.* 7, 77. <https://doi.org/10.1186/1471-2202-7-77>.
20. Toda, T., Parylak, S.L., Linker, S.B., and Gage, F.H. (2019). The role of adult hippocampal neurogenesis in brain health and disease. *Mol. Psychiatry* 24, 67–87. <https://doi.org/10.1038/s41380-018-0036-2>.
21. Gillies, G.E., and McArthur, S. (2010). Estrogen actions in the brain and the basis for differential action in men and women: a case for sex-specific medicines. *Pharmacol. Rev.* 62, 155–198. <https://doi.org/10.1124/pr.109.002071>.
22. Sheppard, P.A.S., Choleris, E., and Galea, L.A.M. (2019). Structural plasticity of the hippocampus in response to estrogens in female rodents. *Mol. Brain* 12, 22. <https://doi.org/10.1186/s13041-019-0442-7>.
23. Chen, Q., Zhang, W., Sadana, N., and Chen, X. (2021). Estrogen receptors in pain modulation: cellular signaling. *Biol. Sex Differ.* 12, 22. <https://doi.org/10.1186/s13293-021-00364-5>.
24. Bean, L.A., Ianov, L., and Foster, T.C. (2014). Estrogen Receptors, the Hippocampus, and Memory. *Neuroscientist* 20, 534–545. <https://doi.org/10.1177/1073858413519865>.
25. Warfvinge, K., Krause, D.N., Maddahi, A., Edvinsson, J.C.A., Edvinsson, L., and Haanes, K.A. (2020). Estrogen receptors  $\alpha$ ,  $\beta$  and GPER in the CNS and trigeminal system - molecular and functional aspects. *J. Headache Pain* 21, 131. <https://doi.org/10.1186/s10194-020-01197-0>.
26. Zhao, L., and Brinton, R.D. (2007). Estrogen receptor  $\alpha$  and  $\beta$  differentially regulate intracellular Ca<sup>2+</sup> dynamics leading to ERK phosphorylation and estrogen neuroprotection in hippocampal neurons. *Brain Res.* 1172, 48–59. <https://doi.org/10.1016/j.brainres.2007.06.092>.
27. Langhnoja, J.M., Buch, L.K., and Pillai, P.P. (2018). 17 $\beta$ -estradiol modulates NGF and BDNF expression through ER $\beta$  mediated ERK signaling in cortical astrocytes. *Biologia* 73, 907–915. <https://doi.org/10.2478/s11756-018-0099-1>.
28. Minichiello, L., Calella, A.M., Medina, D.L., Bonhoeffer, T., Klein, R., and Korte, M. (2002). Mechanism of TrkB-Mediated Hippocampal Long-Term Potentiation. *Neuron* 36, 121–137. [https://doi.org/10.1016/S0896-6273\(02\)00942-X](https://doi.org/10.1016/S0896-6273(02)00942-X).
29. Cannavo, A., Jun, S., Rengo, G., Marzano, F., Agrimi, J., Liccardo, D., Elia, A., Keceli, G., Altobelli, G.G., Marcucci, L., et al. (2023).  $\beta$ 3AR-Dependent Brain-Derived Neurotrophic Factor (BDNF) Generation Limits Chronic Postischemic Heart Failure. *Circ. Res.* 132, 867–881. <https://doi.org/10.1161/CIRCRESAHA.122.321583>.
30. Karisetty, B.C., Joshi, P.C., Kumar, A., and Chakravarty, S. (2017). Sex differences in the effect of chronic mild stress on mouse prefrontal cortical BDNF levels: A role of major ovarian hormones. *Neuroscience* 356, 89–101. <https://doi.org/10.1016/j.neuroscience.2017.05.020>.
31. Guo, L., Chen, Y.-X., Hu, Y.-T., Wu, X.-Y., He, Y., Wu, J.-L., Huang, M.-L., Mason, M., and Bao, A.-M. (2018). Sex hormones affect acute and chronic stress responses in sexually dimorphic patterns: Consequences for depression models. *Psychoneuroendocrinology* 95, 34–42. <https://doi.org/10.1016/j.psyneuen.2018.05.016>.
32. Garrett, J.E., and Wellman, C.L. (2009). Chronic stress effects on dendritic morphology in medial prefrontal cortex: sex differences and estrogen dependence. *Neuroscience* 162, 195–207. <https://doi.org/10.1016/j.neuroscience.2009.04.057>.
33. Bartsch, T., and Wulff, P. (2015). The hippocampus in aging and disease: From plasticity to vulnerability. *Neuroscience* 309, 1–16. <https://doi.org/10.1016/j.neuroscience.2015.07.084>.
34. Mondelli, V., Cattaneo, A., Murri, M.B., Di Forti, M., Handley, R., Hepgul, N., Miorrelli, A., Navari, S., Papadopoulos, A.S., Aitchison, K.J., et al. (2011). Stress and Inflammation Reduce Brain-Derived Neurotrophic Factor Expression in First-Episode Psychosis: A Pathway to Smaller Hippocampal Volume. *J. Clin. Psychiatry* 72, 1677–1684. <https://doi.org/10.4088/JCP.10m06745>.
35. Handa, R.J., Mani, S.K., and Uht, R.M. (2012). Estrogen Receptors and the Regulation of Neural Stress Responses. *Neuroendocrinology* 96, 111–118. <https://doi.org/10.1159/000338397>.
36. Krężel, W., Dupont, S., Krust, A., Chambon, P., and Chapman, P.F. (2001). Increased anxiety and synaptic plasticity in estrogen receptor  $\beta$ -deficient mice. *Proc. Natl. Acad. Sci. USA* 98, 12278–12282. <https://doi.org/10.1073/pnas.221451898>.
37. Kudwa, A.E., McGivern, R.F., and Handa, R.J. (2014). Estrogen receptor  $\beta$  and oxytocin interact to modulate anxiety-like behavior and neuroendocrine stress reactivity in adult male and female rats. *Physiol. Behav.* 129, 287–296. <https://doi.org/10.1016/j.physbeh.2014.03.004>.
38. Hughes, Z.A., Liu, F., Platt, B.J., Dwyer, J.M., Pulicchio, C.M., Zhang, G., Schechter, L.E., Rosenzweig-Lipson, S., and Day, M. (2008). WAY-200070, a selective agonist of estrogen receptor beta as a potential novel anxiolytic/antidepressant agent. *Neuropharmacology* 54, 1136–1142. <https://doi.org/10.1016/j.neuropharm.2008.03.004>.
39. Imwalle, D.B., Gustafsson, J.Å., and Rissman, E.F. (2005). Lack of functional estrogen receptor  $\beta$  influences anxiety behavior and serotonin content in female mice. *Physiol. Behav.* 84, 157–163. <https://doi.org/10.1016/j.physbeh.2004.11.002>.
40. Numakawa, T., Yokomaku, D., Richards, M., Hori, H., Adachi, N., and Kunugi, H. (2010). Functional interactions between steroid hormones and neurotrophin BDNF. *World J. Biol. Chem.* 1, 133–143. <https://doi.org/10.4331/wjbc.v1.i5.133>.
41. Gong, H., Jarzynka, M.J., Cole, T.J., Lee, J.H., Wada, T., Zhang, B., Gao, J., Song, W.-C., DeFranco, D.B., Cheng, S.-Y., and Xie, W. (2008). Glucocorticoids Antagonize Estrogens by Glucocorticoid Receptor-Mediated Activation of Estrogen Sulfotransferase. *Cancer Res.* 68, 7386–7393. <https://doi.org/10.1158/0008-5472.CAN-08-1545>.
42. Chen, H., Lombès, M., and Le Menuet, D. (2017). Glucocorticoid receptor represses brain-derived neurotrophic factor expression in neuron-like cells. *Mol. Brain* 10, 12. <https://doi.org/10.1186/s13041-017-0295-x>.
43. Reingle Gonzalez, J.M., Jetelina, K.K., Olague, S., and Wondrack, J.G. (2018). Violence against women increases cancer diagnoses: Results from a meta-analytic review. *Prev. Med.* 114, 168–179. <https://doi.org/10.1016/j.ypmed.2018.07.008>.
44. Fleischer, A.W., Schalk, J.C., Wetzell, E.A., Hanson, A.M., Sem, D.S., Donaldson, W.A., and Frick, K.M. (2020). Chronic oral administration of a novel estrogen receptor beta agonist enhances memory consolidation and alleviates vasomotor symptoms in a mouse model of menopause: Developing topics. *Alzheimers Dementia* 16, e047645. <https://doi.org/10.1002/alz.047645>.
45. Mersereau, J.E., Levy, N., Staub, R.E., Baggett, S., Zogovic, T., Chow, S., Ricke, W.A., Tagliaferri, M., Cohen, I., Bjeldanes, L.F., and Leitman, D.C. (2008). Ligniritigenin is a plant-derived highly selective estrogen receptor  $\beta$  agonist. *Mol. Cell. Endocrinol.* 283, 49–57. <https://doi.org/10.1016/j.mce.2007.11.020>.
46. Dupuis, M.L., Conti, F., Maselli, A., Pagano, M.T., Ruggieri, A., Anticoli, S., Fragale, A., Gabriele, L., Gagliardi, M.C., Sanchez, M., et al. (2018). The Natural Agonist of Estrogen Receptor  $\beta$  Silibinin Plays an Immunosuppressive Role Representing a Potential Therapeutic Tool in Rheumatoid Arthritis. *Front. Immunol.* 9, 1903. <https://doi.org/10.3389/fimmu.2018.01903>.
47. Kregel, J.H., Hodgin, J.B., Couse, J.F., Enmark, E., Warner, M., Mahler, J.F., Sar, M., Korach, K.S., Gustafsson, J.Å., and Smithies, O. (1998). Generation and reproductive phenotypes of mice lacking estrogen receptor  $\beta$ . *Proc. Natl. Acad. Sci. USA* 95, 15677–15682. <https://doi.org/10.1073/pnas.95.26.15677>.
48. Agrimi, J., Scalco, A., Agafonova, J., Williams Iii, L., Pansari, N., Keceli, G., Jun, S., Wang, N., Mastorci, F., Tichnell, C., et al. (2020). Psychosocial Stress Hastens Disease Progression and Sudden Death in Mice with Arrhythmogenic Cardiomyopathy. *J. Clin. Med.* 9, E3804. <https://doi.org/10.3390/jcm9123804>.
49. Hromadkova, L., Bezdekova, D., Pala, J., Schedin-Weiss, S., Tjernberg, L.O., Hoschl, C., and Ovsepijan, S.V. (2020). Brain-derived neurotrophic factor (BDNF) promotes molecular polarization and differentiation of immature neuroblastoma cells into definitive neurons. *Biochim. Biophys. Acta. Mol. Cell Res.* 1867, 118737. <https://doi.org/10.1016/j.bbamcr.2020.118737>.

## STAR★METHODS

### KEY RESOURCES TABLE

REAGENT or RESOURCE	SOURCE	IDENTIFIER
<b>Antibodies</b>		
Mouse monoclonal anti-ER $\beta$	Santa Cruz Biotechnology	Cat# sc-390243; RRID: AB_2728765
Rabbit polyclonal anti-ER $\beta$	Invitrogen	Cat# PA1-311; RRID: AB_325597
Rabbit polyclonal anti-P-ERK1/2	Cell Signaling Technology	Cat# 9101; RRID: AB_331646
Rabbit polyclonal anti-BDNF	Alomone Labs	Cat# ANT-010; RRID: AB_2039756
Rabbit polyclonal anti-P-TrkB	Millipore	Cat# ABN1381; RRID: AB_2721199
Rabbit polyclonal anti-Doublecortin	Abcam	Cat# ab18723; RRID: AB_732011
Mouse monoclonal anti-BrdU	Cell Signaling Technology	Cat #5292; RRID: AB_10548898
Mouse monoclonal anti-ER $\alpha$	Invitrogen	Cat# MA1-80216; RRID: AB_930763
Chicken polyclonal antibody anti-GAPDH	Sigma-Aldrich	Cat# AB2302; RRID: AB_10615768
<b>Chemicals, peptides, and recombinant proteins</b>		
BrdU	Invitrogen	B23151, CAS 59-14-3
PHTPP	Santa Cruz Biotechnology	CAS 805239-56-9
DPN	MedChemExpress	HY-12452, CAS 1428-67-7
<b>Critical commercial assays</b>		
TUNEL Assay Kits	ThermoFisher	Cat# C10617
17 beta Estradiol ELISA Kit	Abcam	Cat# ab108667
Corticosterone ELISA kit	Abcam	Cat# ab108821
<b>Experimental models: Organisms/strains</b>		
ER $\beta$ KO mice	Jackson Laboratory	Stock #004745
C57BL/6 mice	Charles River	Strain Code 027
CD1 mice	Charles River	Strain Code 022

## RESOURCE AVAILABILITY

### Lead contact

Further information and requests for resources and reagents should be directed to and will be fulfilled by the Lead Contact, Nazareno Paolocci ([npaoloc1@jhmi.edu](mailto:npaoloc1@jhmi.edu)).

### Materials availability

This study did not generate new unique reagents.

### Data and code availability

- All data supporting the findings of this study can be shared by the lead author Nazareno Paolocci upon request.
- No original code has been generated in this study.
- Any additional information required to reanalyze the data reported in this paper is available from the [lead contact](#) upon request.

## EXPERIMENTAL MODEL AND STUDY PARTICIPANT DETAILS

3 to 5-month-old mice were collectively housed in standard cages, in a temperature- and humidity-controlled room under a 12 h light/dark cycle (lights on at 07:00), with *ad libitum* access to food and water. For the studies shown in [Figures 1, 2, 3, and 4](#), C57BL/6 (Charles River, Strain Code 027) and CD1 (Charles River, Strain Code 022) were employed. For the studies shown in [Figure 5](#), we employed 3–5-months-old female ER $\beta$  KO mice (Jackson Laboratory, stock #004745). These mice have been generated by inserting a neomycin resistance gene into exon 3 of the coding gene for ER $\beta$  by using homologous recombination in embryonic stem cells.<sup>47</sup> All animal procedures were carried out according to

the National Institutes of Health (NIH) Guide for the Care and Use of Laboratory Animals. They have been approved by the Institutional Animal Care and Use Committee at Johns Hopkins Medical Institutions (protocol number: MO20M237).

## METHOD DETAILS

### Behavioral tests

#### *Reiterated male-to-female violent interaction*

We employed a recently validated protocol to induce social defeat in female mice<sup>4</sup> [in turn borrowed from the resident-intruder paradigm,<sup>16</sup> widely used to research human psychosocial stress through animal models] to reproduce some salient conditions of human IPV (Figure 1A). In detail, we sprayed a 60  $\mu$ L aliquot of urine collected from a CD1 male mouse on the genital area of a 12–16-weeks-old female C57BL6/J mouse (Figure 1A, first step). Then, we placed the female mouse inside a cage containing a resident aggressive CD1 male mouse. *Selection for the aggressive CD1 male mice.* We pre-selected the dominant CD-1 to maximize the violent component of the interaction. Specifically, before the start of the actual RMFVI paradigm, we selected dominant and highly aggressive CD1s among a large cohort of male mice through daily male-male encounters in which the dominant was singled out and the socially defeated ones excluded, according to the criteria of the classical resident-intruder paradigm<sup>10</sup> (7 days of trials experiment have been performed). As a subsequent step, the dominant males were housed in a single cage and exposed for a week to 10-min encounters daily, with different females treated with male urine. After some rare cases of sexual behavior that occurred in the first encounters, the dominant males showed purely aggressive behavior, with repeated attacks lasting several seconds (we attach a video of the violent behavior). After this training, only the selected aggressive CD-1 males were used for the full RMVA protocol while keeping the same male mouse for a given female one and assigned constantly to the same female. As shown in Figure 1A, the RMFVI procedure triggered a violent reaction by the CD1 resident mouse, manifested in numerous attacks and bites during the 10-min physical interaction. After this step, the two animals were maintained in the same cage for 24 h but physically separated via a perforated transparent plexiglass barrier, thus allowing a continued sensorial connection and, therefore, a psychological threat for the female (step 4). This procedure was repeated for 21 days to induce stress/social defeat. During the 10 min of interaction, the main behavioral parameters linked to aggression and social defeat were recorded (i.e., the frequencies, durations, and latencies of the attacks). The procedure was interrupted in case of physical injuries.

#### *Light-dark box*

The LDB measures anxiety-like behavior in female mice.<sup>12</sup> This test evaluates the innate aversion to open illuminated spaces and the spontaneous exploratory activity of mice. The test apparatus consists of a box separated into a smaller (one-third) dark chamber and a larger (two-thirds) brightly illuminated chamber. Mice were allowed to move freely between the two areas for 5 min while a camera recorded their behavior. The total time spent in the lighted compartment is an index useful for evaluating anxiety-like behavior. At the same time, the number of transitions between the two chambers is an index of exploratory behavior.<sup>48</sup> We selected the mice for testing in random order. After each mouse's performance, the maze was carefully cleaned. The behavioral test was always performed at the same time of day, between 1 p.m. and 4 p.m. The light intensity has been kept consistently around 150 lux.

#### *Elevated plus maze*

The EPM evaluates anxiety-like behavior and locomotor activity in rodents.<sup>12</sup> The test equipment consists of a four-arm maze, two protected by lateral walls (closed arms, 30 cm  $\times$  36.5 cm,  $\times$  15 cm) and the other two exposed (open arms, 30 cm  $\times$  5 cm, 350 lx). EPM exploits the rodent's conflict between aversion to open spaces (i.e., hiding in closed arms of a maze) and instinct to explore new environments (i.e., exploration of open arms of the same maze). The experimental sessions have been videotaped by a camera placed above the apparatus. The analysis of the behavioral parameters was performed using ANY-maze software.

#### *Biochemical assays*

The mice employed for biochemical assays differed from those dedicated to behavioral testing to avoid influencing molecular markers such as corticosterone and BDNF levels.

#### *Immunofluorescence*

Animals were sacrificed with an overdose of ketamine–xylazine solution (K, 100 mg/kg; X, 10 mg/kg) and transcardially perfused with PBS 1X, followed by paraformaldehyde (PFA) 4% solution (Sigma-Aldrich). The brains were removed from the skull, kept in the fixative (PFA 4%) for 24 h, and transferred into PBS 1X. A sliding microtome cut 50  $\mu$ m coronal hippocampus sections in an anteroposterior direction (distance from bregma, rostral to caudal from  $-1.94$  mm to  $-3.64$  mm). For each immunostaining (except for the TUNEL assay), free-floating sections were pretreated with 70% formic acid for 20 min at room temperature (RT). Then the slices were blocked for 1 h at RT with 2% BSA (Thermo Fisher Scientific), incubated overnight at 4°C with primary antibodies (ER $\beta$  1:200 (PA1-311, Thermo Fisher Scientific and sc-390243 Santa Cruz); P-ERK 1:100 (#9101, Cell Signaling); BDNF 1:200, (ANT-010, Alomone Labs); P-TrkB 1:250, (ABN1381, Sigma-Aldrich) and finally incubated with secondary antibodies (1:500, Alexa Fluor, Invitrogen) for 1 h at RT.

### TUNEL assay

TUNEL assay was used to detect hippocampal apoptosis (*In Situ* cell death detection kit; Sigma-Aldrich), as described previously.<sup>16</sup> Percent apoptotic hippocampal cells were calculated via the number of TUNEL-positive nuclei over the total number of hippocampal nuclei per field. At a magnification of 20 $\times$ , five confocal (Leica SP5) images were taken per mouse hippocampus on different z sections covering 20  $\mu$ m.

### Adult neurogenesis

To evaluate adult hippocampal neurogenesis, BrdU (B23151 Invitrogen), was administered intraperitoneally at 75 mg/kg body weight (divided into three different injections every 2 h) the day before starting the RMFVI procedure and evaluated at the end of the 21 days by IF staining. The number of DCX (ab18723, Abcam) and BrdU (mAb #5292, Cell-Signaling) positive cells was estimated in serial coronal sections covering the complete rostrocaudal extension of the DG. At a magnification of 20 $\times$ , five confocal (Leica SP5) images were taken per mouse hippocampus on different z sections covering 20  $\mu$ m). DCX-expressing cells were classified into six distinct groups according to their morphology as previously described<sup>19</sup> (Figure 2F). Briefly, we categorized DCX-expressing cells into 6 categories according to the presence and the shape of apical dendrites and their presumed sequential order. Category A and B were cells with no or very short processes, C and D cells with intermediate length and immature morphology processes, and E and F cells with a more mature appearance. Process length was less than one nucleus-wide (<10  $\mu$ m) in B. In category C, the process was longer than in B, reaching into the granule cell layer but not touching the molecular layer. In category D, the process touched the molecular layer. In groups B, C, and D we often found that the process did not leave the cell perpendicular to the SGZ but had at least an initial segment that went parallel or oblique to the SGZ before curving into the depth of the granule cell layer. In category E, one thick dendrite reached the molecular layer and showed comparatively sparse branching. In category F, the dendritic tree showed delicate branching and few major branches either near the soma or within the granule cell layer. For each DCX-expressing cell, classified as E and F, ImageJ measured the most extended dendrite length.

### Protein expression quantification

For ER $\beta$  and BDNF levels, the following method of quantification was employed: the mean fluorescence intensity within the granular layer and hilus (DG) was quantified using Fiji software (NIH) and with background (the same fluorescent signal belonging to an area selected outside the granular layer and free of DAPI-positive nuclei) subtracted from each image, according to previous studies.<sup>49</sup> Images were acquired via a Leica SP5 confocal microscope.

### Enzyme-linked immune assay

Tissues from the hippocampus and whole brain were dissected and frozen in isopentane. Tissues were homogenized in 2–3 mL of lysis buffer (100 mM PIPES(pH 7), 500 mM NaCl, 0.2% Triton X-100, 2 mM EDTA, 200  $\mu$ M PMSF, and protease inhibitor cocktail (Sigma-Aldrich), followed by centrifugation for 10 min at 16000 g at 4°C. BDNF protein levels were determined by Enzyme-Linked Immune Assay (ELISA) (BDNF Immuno Assay System, Promega). BDNF concentration (pg/mL) was normalized to total soluble protein previously measured through the BCA Protein Assay Kit (Pierce). Blood was collected through the facial vein; E2 and corticosterone levels were determined by ELISA (17-beta-estradiol, ab108667, Abcam; corticosterone, ab108821, Abcam). For circulating markers analysis, we executed the sampling procedure consistently during the female mice diestrus stage.

### Western blot

Proteins were extracted from snap-frozen whole brain and hippocampal samples. We loaded forty micrograms of total protein lysate per lane on 4–20% precast polyacrylamide gel (Mini-PROTEAN TGX, Bio-Rad Laboratories) and blotted electrophoretically. The membrane, including samples was probed with specific antibodies (ER $\beta$  1:500, PA1-311, Invitrogen; ER $\alpha$  1:500, MA1-80216, Invitrogen), and then re-probed for glyceraldehyde 3-phosphate dehydrogenase (GAPDH) with chicken polyclonal antibody, dilution 1:1000 (AB2302, Sigma-Aldrich). Anti-GAPDH antibodies were used to verify the uniformity of protein loading. The protein bands were developed in a chemiluminescence substrate solution (Pierce SuperSignal Chemiluminescent substrate). Analysis of protein bands was performed using ImageJ software (National Institute of Health, USA). We checked the predicted molecular weight using Precision Plus Protein Dual Color Standards (Bio-Rad Laboratories, Inc., Hercules).

### Stereotaxic injections of an estrogen receptor $\beta$ agonist or antagonist in the hippocampus of female mice

The injections were carried out in 4-month-old female C57BL6j mice. Before the procedure, the animals were anesthetized with isoflurane (4% isoflurane induction, 1% isoflurane anesthesia) and placed into a custom-made stereotaxic apparatus. Throughout the procedure, the animals were maintained on a thermostatic blanket at 37°C. An ocular lubricant (Lacrigel, Sunways India Pvt Ltd.) was applied to both eyes, and local anesthesia with 2% lidocaine (ECUPHAR ITALIA SRL) was administered before making an incision in the scalp. After the incision, the skull surface was gently scraped to remove connective tissue, followed by applying hydrogen peroxide (6%) and then 10% iodopovidone (BETADINE Viatrix Inc.). Two small craniotomies (approximately 0.5 mm in diameter each) were drilled on the skull at stereotaxic coordinates [antero-posterior from bregma: –3 mm; medio-lateral: 2 mm] to allow insertion of the micropipette into the tissue (pipette depth: 2 mm from the pia surface). We prepared a dye solution consisting of 30% trypan blue (Merck) in artificial cerebro-spinal fluid (aCSF: containing 127 mM NaCl, 1.0 mM KCl, 1.2 mM KH<sub>2</sub>PO<sub>4</sub>, 26 mM NaHCO<sub>3</sub>, 10 mM D-glucose, 2.4 mM CaCl<sub>2</sub>, 1.3 mM MgCl<sub>2</sub>, and maintained under an atmosphere

of 95% O<sub>2</sub> and 5% CO<sub>2</sub>, with a pH of 7.4). A total volume of 1000 nL of treatment (dye solution and DPN or PHTPP 1 μg/μL) or control solution (i.e., dye solution) was injected at a rate of 100 nL/min at each site using a hydraulic injection apparatus driven by a syringe pump (UltraMicroPump, WPI, Sarasota). Following the procedures, the skull was cleaned, the skin incision sutured, and the area cleansed with 10% iodopovidone. The animals were monitored until fully recovered, and behavioral experiments were conducted 3 h after the injection. No further pharmaceutical treatments were administered to avoid potential undesired interactions with the estrogen pathway.

### QUANTIFICATION AND STATISTICAL ANALYSIS

Results are presented as violin plots. Unpaired t-tests between the control and RMFVI groups analyzed all parametric data. We used the Mann-Whitney U Test for experiments where the sample size was less than six units per group. For the behavioral experiments and the circulating markers (longitudinal study), we employed paired t-tests between baseline and post-treatment. For experiments shown in [Figure 5](#) (4 groups of animals), we used repeated measure ANOVA. All the statistical analyses were conducted through GraphPad PRISM 8.0.2.